



NOVEL ROUTE FOR NANO-SYNTHESIS AND ELECTRICAL PROPERTIES OF FLUORIDE-FREE SILICATE BASED Al^{3+} , Bi^{3+} , AND Cr^{3+} MICA-LIKE CLAYS

Khaled M. Elsabawy^{[a],[b]*}

Keywords: synthesis; Mica clay; fluoride free; XRD; SEM; electrical properties.

Mixed solid state / solution phase routes were applied to synthesize a new family of fluoride-free synthetic clays for water remediation applications. The selected samples of synthetic fluoride-free-Na-4-micas had the general formula of $\text{Na}_4\text{Mg}_6\text{M}_4\text{Si}_4\text{O}_{22}\cdot n\text{H}_2\text{O}$, where $\text{M} = \text{Al}^{3+}$, Bi^{3+} , and Cr^{3+} . Structural and micro-structural properties were determined by using both XRD and SEM. Determining the grain size of the mica, bulk was found to be in the range of 2.37–3.43 μm , which was lower than those reported in the literature. Electrical property investigation proved that Al-clay and Bi-clay exhibited semi-conducting behaviour, but Cr-clay exhibited insulating behaviour. This latter confirmed that the energy gap ΔE_g was the largest for the chromium clay.

* Corresponding Author
E-Mail: ksabawy@yahoo.com

- [a] Materials Science Unit, Chemistry Department, Faculty of Science, 31725-Tanta University, EGYPT.
[b] Materials Science Unit, Faculty of Science, Taif University, Taif City-Alhawyah-888-Saudi Arabia.

1. Introduction

The group of synthetic clays "swelling micas", out of which only one Na-4-mica, were originally developed exclusively for water treatment. They imbibe as they absorb metal ions, then collapse with sealing the metals inside. Na-4-mica is formed by combining kaolinite, a soft clay mineral used in the ceramics industry, with magnesium oxide in sodium fluoride at a temperature of 890°C. The resulting product has sheet like structure (as natural mica's) with brittle composition, but having space between the layers.¹⁻³

Waste effluents in mining operations and various chemical processing industries contain heavy metals which are non-biodegradable and toxic pollutants. Due to their tendency to accumulate in living organisms, causing various diseases and disorders, the treatment methods for metal-containing effluents are essential for environmental and human health protection. Among numerous commonly used techniques for water purification, adsorption techniques have gained much attention because of their cost effectiveness and easy operation.⁴⁻¹⁸

In recent years, an intensive research was conducted focusing on the selection and/or development of low-cost adsorbents with good metal-binding abilities, which could be utilized as an alternative to the most widely used adsorbent, activated carbon in wastewater treatment. Natural materials of both organic and inorganic nature (such as chitosan, zeolites, minerals, etc.) and certain waste products from industrial operations (such as fly ash, coal and oxides)

are already classified as low-cost adsorbents because of their local availability and economic nature.¹⁹⁻²⁸

The major objective of the present article is to investigate the effect of solution route synthesis on

- the structural and nano-structural properties of $\text{Na}_4\text{Mg}_6\text{M}_4\text{Si}_4\text{O}_{22}\cdot n\text{H}_2\text{O}$ mica clay samples, and on
- the electrical properties of $\text{Na}_4\text{Mg}_6\text{M}_4\text{Si}_4\text{O}_{22}\cdot n\text{H}_2\text{O}$ mica clay samples.

2. Experimental section

2.1. Sample preparation

The selected samples of synthetic fluoride-free-Na-4-mica with the general formula of $\text{Na}_4\text{Mg}_6\text{M}_4\text{Si}_4\text{O}_{22}\cdot n\text{H}_2\text{O}$, where $\text{M} = \text{Al}^{3+}$, Bi^{3+} , or Cr^{3+} , were synthesized by applying solution phase route and sintering procedure using the molar ratios of highly pure $\text{Na}_2\text{O}\cdot 2\text{SiO}_2\cdot 2\text{H}_2\text{O}$, MgCO_3 , Al_2O_3 , Bi_2O_3 , and Cr_2O_3 . Mixtures were grounded carefully, then they were dissolved in concentrated nitric acid to form nitrate extract, which was then diluted with distilled water. The nitrate solution was then neutralized by using 45 % urea solution with pH ~ 6.5.

A sodium silicate solution was prepared first and noted as Mixture I. Another solution, mixture II, contained the required Al-, Mg-, Bi-, and Cr-nitrates according to the desired chemical formula. The pH of Mixture I was adjusted to 8.5, then a concentrated solution of ammonia was added carefully until thick white precipitate of metal hydroxides were obtained, according to the fact that pH must be higher than 8. The precursor is filtered, and washed with 2.5 % ammonium nitrate solution. Mixture II containing Al-, Mg-, Bi-, and Cr-salts was passed through the same treatment but in the presence of ethylene glycol as complexing agent in order to produce gelatinous precipitate of metal cation hydroxide precursors.

Precursors, Mixture I + II, were placed into a muffle furnace for calcination process at 880 °C under a compressed air atmosphere for 15 hours, then re-grounded and pressed into pellets (thickness 0.2 cm and diameter 1.2 cm) under 10 Tons/cm². Sintering was carried out under air stream at 1050 °C for 10 hours. Samples were slowly cooled down (20 °C/hour) till 500 °C and annealed there for 5 hours under air stream. The furnace was shut off and cooled slowly down to room temperature. Finally, the product materials were kept in vacuum desiccators over silica gel dryer.

The synthesized samples were named as Clay I ($\text{Na}_4\text{Mg}_6\text{Al}_4\text{Si}_4\text{O}_{22}\cdot n\text{H}_2\text{O}$), Clay II ($\text{Na}_4\text{Mg}_6\text{Bi}_4\text{Si}_4\text{O}_{22}\cdot n\text{H}_2\text{O}$), and Clay III ($\text{Na}_4\text{Mg}_6\text{Cr}_4\text{Si}_4\text{O}_{22}\cdot n\text{H}_2\text{O}$). As shown in Fig. 1, tetrahedral units of silicate forms the backbone of mica clay structure, indicating that each unit cell is surrounded by 4-Na-atoms that can be replaced if it is applied as cation exchanger.

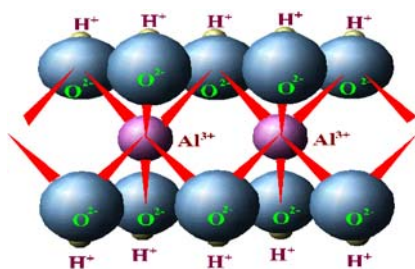


Figure 1. Structure of Al-silicates – Clay I

2.2. Phase identification

The X-ray diffraction (XRD) measurements were carried out at room temperature on fine ground samples using Cu-K_α radiation source, Ni-filter, and a computerised STOE diffractometer from Germany with two theta step scan technique.

Scanning Electron Microscopy (SEM) measurements were carried out at different sectors in the prepared samples by using a computerized SEM camera with elemental analyzer unit (PHILIPS-XL 30 ESEM from USA).

2.3. Electrical measurement

DC-electrical conductivities of prepared materials were recorded as a function of temperature from room temperature up to 520 °C, and measurements were performed on the pellet surface by using two probe circuit and graphite paste as connective matter.

3. Results and discussion

3.1. Phase identification

Fig. 2 displays the X-ray powder diffraction patterns recorded for synthetic fluoride-free-Na-4-mica samples with the general formula of $\text{Na}_4\text{Mg}_6\text{M}_4\text{Si}_4\text{O}_{22}\cdot n\text{H}_2\text{O}$, where $\text{M} = \text{Al}^{3+}$, Bi^{3+} , and Cr^{3+} . The analysis of corresponding 2θ values and inter-planer spaces d (Å) were carried out using a

computerized program. This latter indicated that the X-ray crystal structure mainly belongs to a monoclinic phase $\text{Na}_4\text{Mg}_6\text{M}_4\text{Si}_4\text{O}_{22}\cdot n\text{H}_2\text{O}$ in major, besides few peaks of unreacted starting oxides as secondary phase in minor. The lattice parameters of the unit cell were refined using the least-squares sub-routine on a standard computer program. These refined lattice parameters were found typically to those reported in references [19-23]. These unit cell parameters are in good agreement with those reported for $\text{Na}_4\text{Mg}_6\text{M}_4\text{Si}_4\text{O}_{22}\cdot n\text{H}_2\text{O}$.⁶

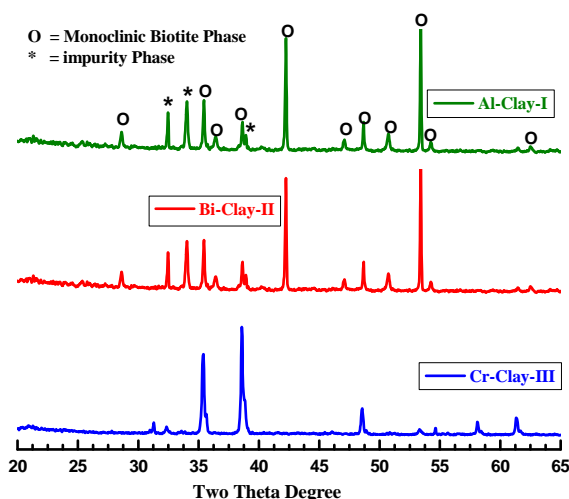


Figure 2. X-ray diffraction patterns for Al-clay (Clay I, top), Bi-clay (Clay II, middle), and Cr-clay (Clay III, bottom)

It is obviously that the addition of nano-oxide components has a negligible effect on the main crystalline structure of $\text{Na}_4\text{Mg}_6\text{M}_4\text{Si}_4\text{O}_{22}\cdot n\text{H}_2\text{O}$ with fluoride content ($x = 0.0$) as shown in Fig. 2 (bottom).

From Fig. 2 (top and middle) one can interpret that the monoclinic phase of mica-clay $\text{Na}_4\text{Mg}_6\text{M}_4\text{Si}_4\text{O}_{22}\cdot n\text{H}_2\text{O}$ is the dominating phase, which exceeds 90% ($d_{100} = 1.12\text{-}1.13$ nm), confirming that nano-oxide component are successfully reacted and formed monoclinic biotite phase with a good degree of crystal nature.

EDX analysis indicated that the atomic percentage recorded is a bit typical for the molar ratios of the prepared sample, emphasizing the quality of preparation through solution technique.

On the basis of molar ratio, the allowed error in experimental procedures throughout solution route is smaller than those reported in literatures for samples synthesized by solid state routes.^{1,27}

3.2. SE-microscopy measurements

Fig. 3-5 show SEM-micrographs recorded for $\text{Na}_4\text{Mg}_6\text{M}_4\text{Si}_4\text{O}_{22}\cdot n\text{H}_2\text{O}$, where $\text{M} = \text{Al}^{3+}$, Bi^{3+} , and Cr^{3+} , prepared via solution route. The estimated average of grain size was calculated and found to be in the region of 2.37 – 3.43 μm supporting the data already reported in ref. [23].

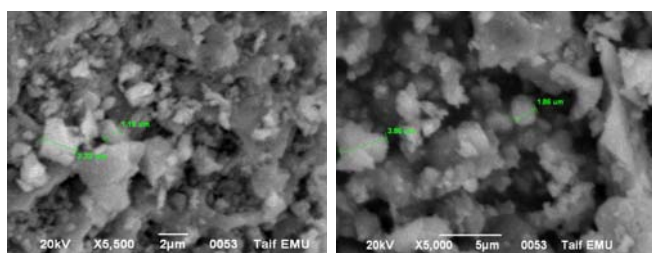


Figure 3. SE-micrographs recorded for Al-clay-I with different magnification factors

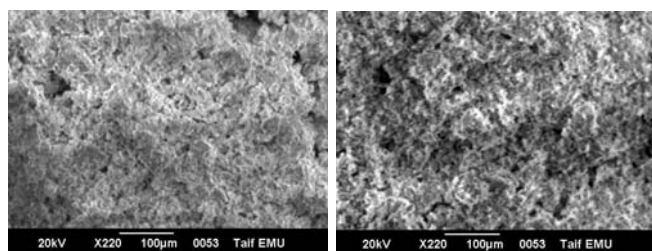


Figure 4. SE-micrographs recorded for Bi-clay-II with different magnification factors

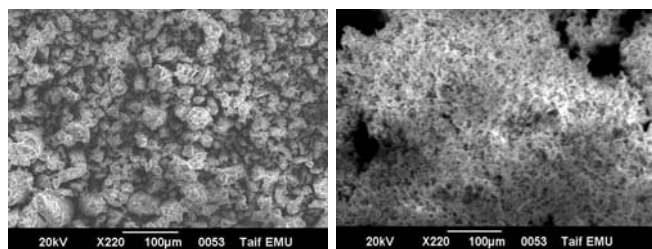


Figure 5. SE-micrographs recorded for Cr-clay-III with different magnification factors

The EDX examinations for random spots in the same sample confirmed and are also consistent with our XRD analysis for polycrystalline $\text{Na}_4\text{Mg}_6\text{M}_4\text{Si}_4\text{O}_{22}\cdot n\text{H}_2\text{O}$, which was prepared via solution route, so that the differences in the molar ratios estimated by EDX for the same sample is emphasized as an evidence for the existence of monoclinic phase with good approximation to molar ratios.

It is difficult to observe inhomogeneity in Fig. 3-5 within the micrograph due to the fact that powders used are very fine and the particle size estimated is too small. This indicates, that the actual grain size in the material bulk is smaller than that detected on the surface morphology. Furthermore, particle size was estimated from both XRD and SEM analyses and its average was found to be between 25 and 124 nm, confirming that solution route synthesis increases the fraction ratio of nano-particle formation.

3.3. Electrical properties

Fig. 6 shows the DC-electrical conductivity of the prepared mica-materials $\text{Na}_4\text{Mg}_6\text{M}_4\text{Si}_4\text{O}_{22}\cdot n\text{H}_2\text{O}$, which was recorded as a function of temperature from room temperature up to 520 °C, and performed on the pellet surface by using two probe circuit and graphite paste as connective matter.

It is clear that the conduction increases as temperature raises reflecting semiconductor behaviour for both Al-clay-I and Bi-clay-II samples, while insulating behaviour for Cr-clay-III sample.

Although most of mineral silicate-structure clays in the literature are semiconductors,²²⁻²⁵ Cr-clay-III was found to has an insulating behaviour through the investigated temperature range, reflecting the larger energy gap for Cr-clay-III.

Transport properties of the materials obeys the Arrhenius equation $\sigma_{ac} = \sigma_0 \cdot \exp(-E_a/K_B T)$, where the symbols have their usual meanings. It is observed that the conductivity of the material increases with the increase of the temperature, and shows the negative temperature coefficient of resistance behaviour for both clay I and clay II. The calculated values of activation energies of the clay compounds are 0.34, 0.41, and 1.39 eV for Clay I, Clay II, and Clay III, respectively. This behaviour suggests that the conduction mechanism of the investigated compounds may be due to charge carrier which enhanced by cation holes, and the energy gap between the conduction and valence band increases from clay I to clay III.

From Fig. 6 it is clear that Bi-clay-II exhibits semi-conducting behaviour up to 410 °C and loose its semi-conducting behaviour above this temperature due to an increase in its energy gap, which results in an insulating behaviour as shown in Fig. 6.

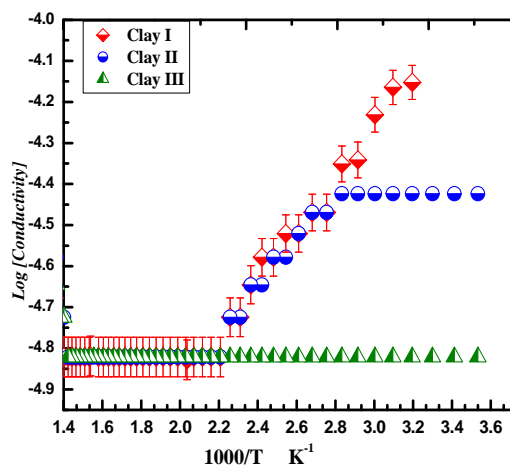


Figure 6. DC-electrical conductivity for Clay I, Clay II, and Clay III as a function of absolute temperature

4. Conclusion

The conclusive remarks of the present article can be summarized as follows:

1. solution phase technique exhibits structure quality as a preparation technique,
2. synthetic fluoride-free $\text{Na}_4\text{Mg}_6\text{M}_4\text{Si}_4\text{O}_{22}\cdot n\text{H}_2\text{O}$ crystallizes in monoclinic phase,
3. SE-micrographs confirmed that particle size was in nano-scale (25-135 nm),
4. Clay-III ($\text{Na}_4\text{Mg}_6\text{M}_4\text{Si}_4\text{O}_{22}\cdot n\text{H}_2\text{O}$, where $M = \text{Cr}^{3+}$) has the highest E_g value of 1.39 eV.

5. References

- ¹ Komarneni, S. and Ravella, R. *Current Applied Physics*, **2008**, *8*, 104-106.
- ² Adebowale, K.O., Unuabonah, I.E. and Olu-Owolabi, B.I. *Journal of Hazardous Materials B*, **2006**, *134*, 130-139.
- ³ Al-degs, Y., Khraisheh, M.A.M. and Tutunji, M.F. *Water Research*, **2009**, *35*, 3724-3728.
- ⁴ Al-Ghouti, M.A., Khraisheh, M.A.M. and Tutunji, M. *Chemical Engineering Journal*, **2004**, *104*, 83-91.
- ⁵ Allen, S.J. and Koumanova, B. *Journal of Chemical Technology and Metallurgy*, **2005**, *40*, 175-192.
- ⁶ Aytas, S., Akyil, S., Aslani, M.A.A. and Aytakin, U. *Journal of Radioanalytical and Nuclear Chemistry*, **1999**, *240*, 973-976.
- ⁷ Babel, S. and Kurniawan, T.A. *Journal of Hazardous Materials B*, **2003**, *97*, 219-243.
- ⁸ Barrett, E.P., Youner L.G. and Halenda, P. *Journal of the American Chemical Society*, **1951**, *73*, 373-380.
- ⁹ Bhattacharyya, K.G. and Gupta, S.S. *Journal of Colloid and Interface Science*, **2007**, *310*, 411-424.
- ¹⁰ Camilo C., Carmen G. and Paula M. *Journal of Chemical Technology & Biotechnology*, **2005**, *80*, 477-481.
- ¹¹ Charnock, J.M., England, K.E.R., Farquhar, M.L. and Vaughan, D.J. *Physica. B, Condensed Matter*, **1995**, *208-209*, 457-458.
- ¹² Dantas, T.N.D., Neto, A.A.D. and Moura, M.C.P. *Water Research*, **2001**, *35*, 2219-2224.
- ¹³ Doula, M.K. and Ioannou, A. *Microporous and Mesoporous Materials*, **2003**, *58*, 115-130.
- ¹⁴ Ekmekyapar, F., Aslan, A., Bayhan, Y.K. and Cakici, A. *Journal of Hazardous Materials*, **2006**, *137*, 293-298.
- ¹⁵ Erdem, E., Karapinar, N. and Donat, R. *Journal of Colloid and Interface Science*, **2004**, *280*, 309-314.
- ¹⁶ Hamdaouia, O. and Naffrechoux, E. *Journal of Hazardous Materials*, **2007**, *147*, 381-394.
- ¹⁷ Ho, Y.S., Porter, J.F. and McKay, G. *Water, Air, and Soil Pollution*, **2002**, *141*, 1-33.
- ¹⁸ IPCS (International Programme on Chemical Safety) 1998. Copper. Environmental Health Criteria 200. Geneva, Switzerland: World Health Organization, **1998**.
- ¹⁹ Kayaa, A. and Oren, A.H. *Journal of Hazardous Materials B*, **2005**, *125*, 183-189.
- ²⁰ Khraisheh, M.A.M., Al-degs, Y.S. and Mcminn W.A.M., *Chemical Engineering Journal*, **2004**, *99*, 177-184.
- ²¹ Kubilay, S., Gürkan, R., Savran, A. and Şahan, T., *Adsorption*, **2007**, *13*, 41-51.
- ²² Lazarević, S., Janković-Častvan, I., Jovanović, D., Milonjić, S., Janačković, Dj. and Petrović, R. *Applied Clay Science*, **2007**, *37*, 47-57.
- ²³ Lin, S.-H. and Juang, R.-S. *Journal of Hazardous Materials B*, **2002**, *92*, 315-326.
- ²⁴ Meunier, N., Laroulandie, J., Blais, J.F. and Tyagi, R.D. *Bioresource Technology*, **2003**, *90*, 255-263.
- ²⁵ Mishra, T. and Tiwari, S.K. *Journal of Hazardous Materials B*, **2006**, *137*, 299-303.
- ²⁶ Osmanlioglu, A.E. *Applied Radiation and Isotopes*, **2007**, *65*, 17-20.
- ²⁷ Panayotova, M. and Velikov, B. *Journal of Environmental Science and Health*, **2002**, *A 37*, 139-147.

Received: 08.10.2012.
Accepted: 22.10.2012.